

# Mechanical Properties and Morphology of Polypropylene-Calcium Carbonate Nanocomposites Prepared by Dynamic Packing Injection Molding

Xueqin Gao, Cong Deng, Chao Ren, Jie Zhang, Zhongming Li, Kaizhi Shen

Department of Polymer Processing, College of Polymer Science and Engineering, The State Key Laboratory of Polymer Materials Engineering, Sichuan University, Chengdu, Sichuan 610065, People's Republic of China

Received 28 October 2009; accepted 26 May 2011

DOI 10.1002/app.34982

Published online 18 October 2011 in Wiley Online Library (wileyonlinelibrary.com).

**ABSTRACT:** In this article, dynamic packing injection molding (DPIM) technology was used to prepare injection samples of Polypropylene-Calcium Carbonate (PP/CaCO<sub>3</sub>) nanocomposites. Through DPIM, the mechanical properties of PP/nano-CaCO<sub>3</sub> samples were improved significantly. Compared with conventional injection molding (CIM), the enhancement of the tensile strength and impact strength of the samples molded by DPIM was 39 and 144%, respectively. In addition, the tensile strength and impact strength of the PP/nano-CaCO<sub>3</sub> composites molded by DPIM increase by 21 and 514%, respectively compared with those of pure PP through CIM. According to the SEM, WAXD, DSC measurement, it could be found

that a much better dispersion of nano-CaCO<sub>3</sub> in samples was achieved by DPIM. Moreover,  $\gamma$  crystal is found in the shear layer of the DPIM samples. The crystallinity of PP matrix in DPIM sample increases by 22.76% compared with that of conventional sample. The improvement of mechanical properties of PP/nano-CaCO<sub>3</sub> composites prepared by DPIM attributes to the even distribution of nano-CaCO<sub>3</sub> particles and the morphology change of PP matrix under the influence of dynamic shear stress. © 2011 Wiley Periodicals, Inc. *J Appl Polym Sci* 124: 1392–1397, 2012

**Key words:** dynamic packing injection molding (DPIM); nanocomposites; mechanical properties; morphology

## INTRODUCTION

Calcium Carbonate (CaCO<sub>3</sub>) is widely used as a kind of inorganic filler in the plastics industry because of its low price and rich resource. Nanoparticles of CaCO<sub>3</sub> can toughen and strengthen polymer because nano-CaCO<sub>3</sub> has some special features and effect.<sup>1–3</sup> Polypropylene has better comprehensive performance except its poor impact toughness. Therefore, many researchers have worked on modified PP by filling nano-CaCO<sub>3</sub> particles to improve toughness of PP.<sup>4–9</sup> Most research is focused on the surface modification of nanoparticles to improve the dispersion of nano-CaCO<sub>3</sub> particles. The study of Wan<sup>10</sup> shows that the mechanical properties of PP/nano-CaCO<sub>3</sub> composites through surface modification can be improved to a certain degree compared with that of pure PP. The tensile strength increases by 4.26% and the impact strength increases by 16.46%. The best content of nano-CaCO<sub>3</sub> particles is 4%.<sup>11</sup> When the

content of nano-CaCO<sub>3</sub> particles exceeds 4%, the tensile strength of the composites will decrease because of the agglomerated nanoparticles.<sup>12</sup> It is well known that the dispersive ability of nanoparticles is crucial to obtain composites with high performance. In this article, we intend to use the dynamic shear stress of dynamic packing injection molding (DPIM)<sup>13</sup> device to improve the dispersion of nano-CaCO<sub>3</sub> particles in PP and change the morphology of PP matrix except treating nano-CaCO<sub>3</sub> particles by silane coupling agent. The content of nano-CaCO<sub>3</sub> particles is set at 9% to reduce cost. The mechanical properties of PP/nano-CaCO<sub>3</sub> composites samples obtained by DPIM are studied to test the effect of DPIM technology. The results show that the tensile strength and impact strength of the PP/nano-CaCO<sub>3</sub> composites molded by DPIM increase by 21 and 514.43%, respectively compared with those of pure PP through CIM. Compared with conventional injection molding, the enhancement of the tensile strength and impact strength of the samples molded by DPIM was 39 and 144%, respectively. The enhancement of mechanical properties of samples through DPIM is greatly higher than that of samples only through surface treatment and that of pure PP. This shows that DPIM technology is very effective to improve mechanical properties of PP/nano-CaCO<sub>3</sub> composites.

Correspondence to: S. Kaizhi (gxqsnow@163.com).

Contract grant sponsor: National Natural Science Fund of China; contract grant numbers: 50803038, 50873072, 50903054.

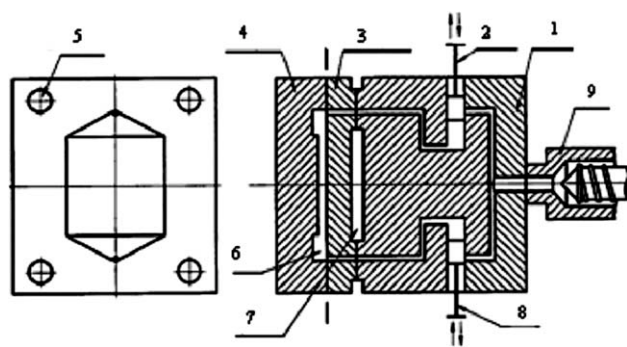


**Figure 1** Dynamic packing injection molding device. (1) double live-feed device; (2) piston A; (3) stationary plate; (4) moving plate; (5) guide pin; (6) cavity; (7) insulating air layer; (8) piston B; (9) injection molding machine.

## EXPERIMENTAL

### Materials

The materials used in this work were iPP (F401, Lanzhou Petrochemical corporation, China) with a melt flow rate of 2.5 g/10 min measured at 190°C under 2.16 kg, and nano-CaCO<sub>3</sub> (treated by silane coupling agent) with an average grain diameter of 50–70 nm.

### Sample preparation

Nano-CaCO<sub>3</sub> particles should be dried for 4 h at 80°C in baking oven owing to its hydrophilicity firstly. Then, PP particles and nano-CaCO<sub>3</sub> particles matched with mass ratio of 10 : 1 were pelletized by corotating intermeshing twin-screw extruder. Granules achieved should be dried for 4 h at 80°C in baking oven before they were put into the dynamic packing injection molding (DPIM) device. The schematic diagram of DPIM device was shown in Figure 1. The DPIM device make the polymer melt get shear action by the reciprocal motion of the piston A and B. The piston A and B of the hydraulic cylinder were controlled by the hydraulic system of injection molding machine. The basic processing parameters for DPIM are listed in Table I. When the oscillation pressure of cylinder is 0 MPa, the experimental device was equivalent to a conventional injection

**TABLE I**  
Basic Processing Parameters for DPIM

Processing parameter	Parameter value
Basic injection pressure	6 MPa
Oscillation pressure of cylinder	0 MPa, 10 MPa, 11 MPa, 12 MPa, 13 MPa
Melt temperature	210°C
Mold temperature	30°C
Oscillation frequency	0.2 Hz

molding (CIM) machine. The specimens was designed to be a 60 × 60 × 4 mm<sup>3</sup> thin square plate with two thickened fan gates (Fig. 2).

### Impact testing (GB/T 1043-93)

Square plates (60 × 60 × 4 mm<sup>3</sup>) obtained after cutting off the two fan gates of the specimens were cut into rectangle plates (60 × 10 × 4 mm<sup>3</sup>) along the parallel or vertical to the flow direction. The rectangle plates as impact specimens were V-type notched using a cutter (XQZ-1). An Izod impact machine (UJ-40) was used to measure the impact strength of samples at room temperature. Four samples were tested per set for impact testing. Standard deviation is less than 5 KJ/m<sup>2</sup>.

### Tensile testing (ASTM D638M)

Dumbbell specimens were obtained from aforementioned rectangle plates by milling processes. A universal electronic testing machine (REGER-3010) was used for tensile testing at room temperature (23°C), at a crosshead speed of 50 mm min<sup>-1</sup>. Four samples were tested per set for tensile testing. Standard deviation is less than 2 MPa.

### Scanning electron microscopy measurements

The cross-section morphology of the samples was studied with an X-650 Hitachi scanning electron microscope (SEM). The acceleration voltage used for

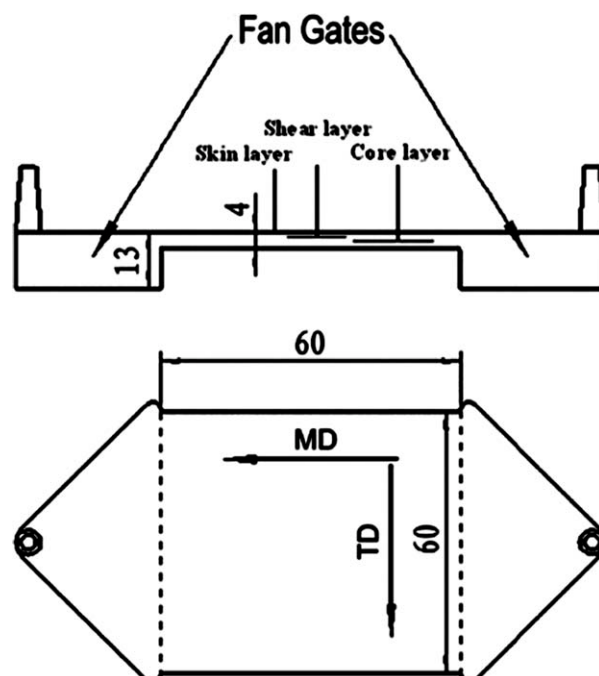


**Figure 2** Outline of the square plate specimen. Dimensions are given in millimeters.

SEM is 20 kV. Brittle fracture samples were obtained after freezing by liquid nitrogen. The brittle fracture surface was sputtered with thin layer gold before the SEM analysis.

### Wide-angle X-ray diffraction measurements

Wide-angle X-ray diffraction (WAXD) experiments were conducted using a Philips X'Pert Pro diffractometer. The shear layer (1 mm from the surface layer) was ground and polished prior to being measured.

### Differential scanning calorimetry measurements

The differential scanning calorimetry (DSC) measurements were performed on slices about 0.5 mm in thickness taken from the oriented zones 1 mm below the original surface of the samples. The tests were conducted using a NETZSCH DSC 204 F1 differential scanning calorimeter, which scanned at  $10^{\circ}\text{C min}^{-1}$ . The weight of samples each testing was around 5 mg. During the measurement, dried nitrogen gas was purged at a constant flow rate.

## RESULTS AND DISCUSSION

### Mechanical properties

#### Tensile strength influenced by oscillation pressure

Figure 3 shows changes of tensile strength of PP and PP/nano- $\text{CaCO}_3$  samples with oscillation pressure in the flow direction of polymer melt during the course of processing. The oscillation pressure means the cylinder pressure made piston vibrate. For the CIM samples (when the pressure is zero), the tensile strength of PP (42.88 MPa) is obviously higher than that of PP/nano- $\text{CaCO}_3$  composites (37.25 MPa). This might be because nano- $\text{CaCO}_3$  particles are easy to agglomerate owing to their big surface energy. These agglomerated particles as weak spot of material mechanical properties can cause a decline in performance.

With increase of oscillation pressure, tensile strengths of PP and PP/nano- $\text{CaCO}_3$  composites all increase notably. For PP, the maximum tensile strength of DPIM is 50.93 MPa, a 19% increase compared with that of CIM (42.88 MPa). Chen LM *et al.*<sup>14</sup> found that the morphology of DPIM samples was shish-kebab interlocking structure. Moreover, the WAXD measurement indicated that  $\beta$  crystal and  $\gamma$  crystal formed in the DPIM samples. The improvement of the tensile strength of PP might attribute to the formation of  $\gamma$  crystal. For PP/nano- $\text{CaCO}_3$ , the maximum tensile strength of DPIM is 51.74 MPa, a 39% increase compared with that of CIM (37.25 MPa). The increase of the tensile strength of PP/

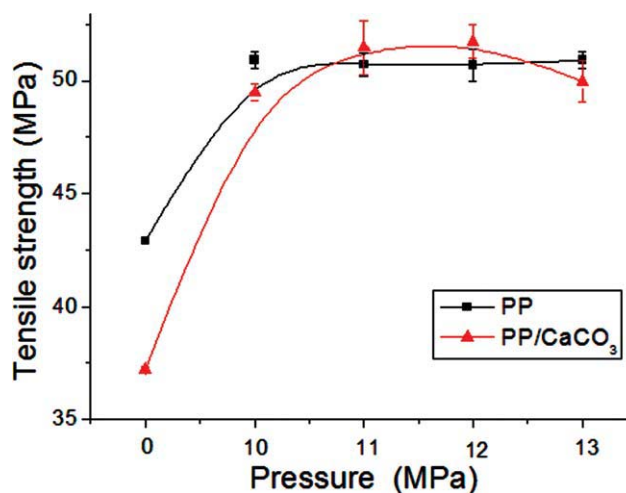


**Figure 3** Tensile strength curves of PP and PP/nano- $\text{CaCO}_3$  samples. [Color figure can be viewed in the online issue, which is available at [wileyonlinelibrary.com](http://wileyonlinelibrary.com).]

nano- $\text{CaCO}_3$  composites compared with that of CIM (39%) improves more greatly than that of pure PP (19%). In addition, the tensile strength of PP/nano- $\text{CaCO}_3$  composites through DPIM increases by 21% compared with that of pure PP through CIM. This shows that DPIM technology can improve the tensile strength of PP/nano- $\text{CaCO}_3$  composites effectively.

From the error bar in Figure 3, we can see that the data difference between PP and PP/ $\text{CaCO}_3$  through DPIM is basically in range of experimental error. As for pure PP, the improvement of the tensile strength might attribute to the change of morphology and crystal. As for PP/nano- $\text{CaCO}_3$  composites, the strong dynamic shear field can make the nano- $\text{CaCO}_3$  particles aggregate difficultly and disperse evenly besides inducing the change of PP matrix crystal structure. The mechanical weak spots caused by agglomerated particles lessen greatly due to the even dispersion of nano- $\text{CaCO}_3$  particles. Negative influence of agglomerated particles is greatly reduced. Thus, the tensile strength of PP/nano- $\text{CaCO}_3$  composites improves distinctly and come up to the tensile strength of PP through DPIM.

#### Impact strength influenced by oscillation pressure

Figure 4 shows changes of impact strength of PP and PP/nano- $\text{CaCO}_3$  samples with oscillation pressure. From Figure 4, it can be seen that the impact strength of PP/nano- $\text{CaCO}_3$  composites ( $48.85 \text{ KJ m}^{-2}$ ) improves more obviously than that of PP ( $19.4 \text{ KJ m}^{-2}$ ) for CIM samples. This might be because that the nano- $\text{CaCO}_3$  particles can induce PP matrix to produce plentiful craze-shear ribbons which consume some impact energy when samples are impacted. Moreover, the presence of nano- $\text{CaCO}_3$  particles can make the crack of PP matrix end.

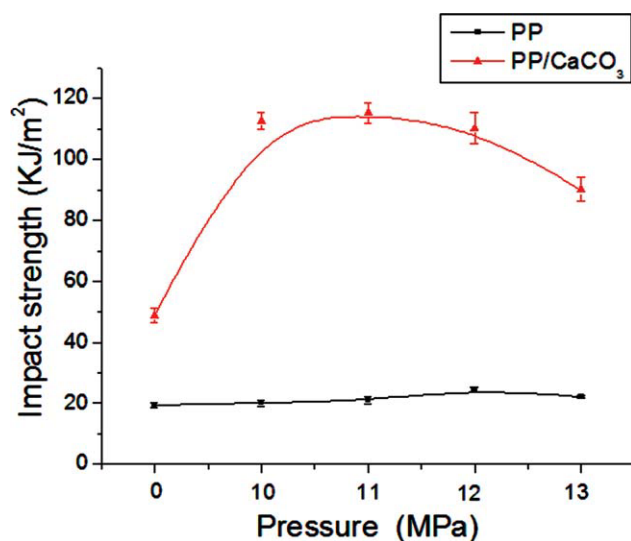


**Figure 4** Impact strength curves of PP and PP/nano-CaCO<sub>3</sub> samples. [Color figure can be viewed in the online issue, which is available at [wileyonlinelibrary.com](http://wileyonlinelibrary.com).]

With increase of oscillation pressure, impact strengths of PP/nano-CaCO<sub>3</sub> composites increase notably compared with that of PP. The maximum impact strength of PP/nano-CaCO<sub>3</sub> composites is 119.18 KJ m<sup>-2</sup>, an 144% increase compared with the conventional strength (48.85 KJ m<sup>-2</sup>), and the maximum impact strength of PP is 24.53 KJ m<sup>-2</sup>, a 26% increase compared with the conventional strength (19.4 KJ m<sup>-2</sup>). The impact of PP/nano-CaCO<sub>3</sub> composites through DPIM increased by 514% compared with that of pure PP through CIM. This might be because that dynamic shear field makes the nano-CaCO<sub>3</sub> particles disperse more uniformly. Toughening effect of the nano-CaCO<sub>3</sub> particles heighten accordingly. Thus, the impact strength of PP/nano-CaCO<sub>3</sub> samples improves more distinctly.

Modulus and elongation at break influenced by oscillation pressure

Table II shows changes of elongation at break and modulus of PP/nano-CaCO<sub>3</sub> samples with oscillation pressure. It can be seen that elongation at break of DPIM samples is less than that of CIM samples. It might attribute to the orientation of PP matrix caused by shear stress which is not favorable to elongation at break. In addition, modulus of DPIM samples increase compared with that of CIM samples. This might mainly attribute to the increase of crystallinity caused by even dispersion of nanoparticles and orientation of matrix PP.

SEM analysis

Figure 5 shows SEM photographs with magnification of 2500 and 5000 of PP/nano-CaCO<sub>3</sub> specimen's

brittle fraction surfaces under CIM and DPIM. There are many nano-CaCO<sub>3</sub> agglomerated particles in CIM sample. These agglomerated particles can cause stress concentration, and become weak spot of material mechanical properties. However, nano-CaCO<sub>3</sub> particles disperse much better in DPIM sample. The dispersive quality of the nanometer inorganic particles in the matrix is crucial to toughening and strengthening of the polymer base inorganic nanocomposites. The even dispersion of nano-CaCO<sub>3</sub> particles make the impact strength and tensile strength of DPIM PP/nano-CaCO<sub>3</sub> specimens improve more obviously compared with that of CIM specimens. This also validates the foregoing conjecture about the reason of mechanical properties improvement of samples obtained by DPIM.

WAXD measurements

Figure 6 shows WAXD curves of CIM and DPIM samples shear layer. The incisive diffraction peaks at 14.2, 17.1, and 18.6° correspond separately to characteristic diffraction peak of the matrix PP  $\alpha$  crystal (110), (040), and (130) crystal face.<sup>15,16</sup> The diffraction peak at about 16° corresponds to characteristic diffraction peak of the matrix PP  $\beta$  crystal (300) crystal face. Only small  $\beta$  crystal diffraction peaks present in both CIM and DPIM samples. This indicates that  $\beta$  crystal is less influenced by the strong shear action. The diffraction peak at about 21° corresponds to characteristic diffraction peak of the matrix PP  $\gamma$  crystal (117) crystal face. The  $\gamma$  crystal is not found in the CIM samples. However, there is evident  $\gamma$  crystal diffraction peak in the DPIM samples. This shows strong shear action is favorable to the formation of  $\gamma$  crystal. The formation of  $\gamma$  crystal is helpful to the improvement of Young's modulus and tensile strength.<sup>17,18</sup> It is known from the aforementioned mechanical properties test that the tensile strength of DPIM samples is higher than that of CIM samples. We think that the formation of  $\gamma$  crystal under the dynamic shear field is one of the reasons for the improvement of tensile strength of the DPIM samples.

DSC measurements

Figure 7 shows DSC curves of CIM and DPIM samples. DSC analysis can be used to obtain the crystal

**TABLE II**  
Modulus and Elongation at Break of PP/CaCO<sub>3</sub> Influenced by Oscillation Pressure

Pressure (MPa)	0	10	11	12	13
Elongation at break (%)	155.28	134.06	114.67	134.38	119.81
Modulus (MPa)	241.28	277.50	311.75	261.29	266.27

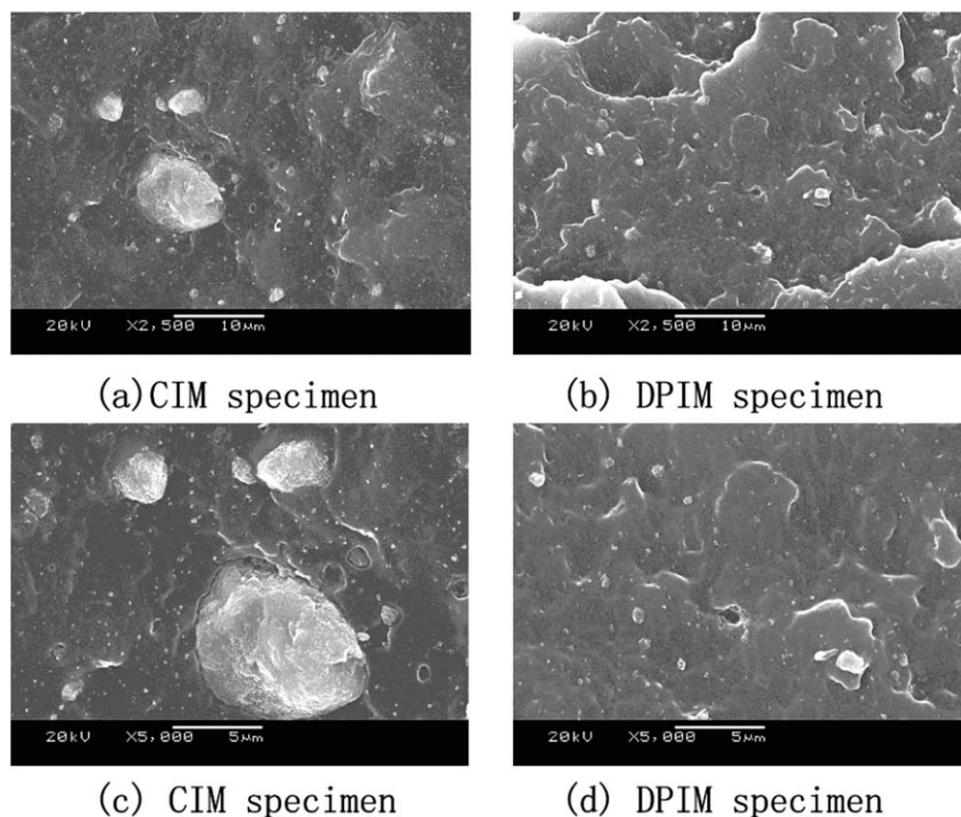


Figure 5 SEM photographs of PP/nano-CaCO<sub>3</sub> specimens under CIM and DPIM.

fusion heat of PP in PP/nano-CaCO<sub>3</sub> composites. The crystallinity of sample can be calculated by the following equation:

$$X_c = \{ \Delta H_C / [(1 - \Phi) \Delta H_m^0] \} \times 100\%,$$

where  $X_c$  is the crystallinity of sample,  $\Delta H_C$  is the measured crystal fusion heat of sample from DSC

thermogram,  $\Phi$  is the mass percent of nano-CaCO<sub>3</sub> in sample, and  $\Delta H_m^0$  is a perfect crystal fusion heat of PP (209 J g<sup>-1</sup>). The temperature of melting peak for PP/nano-CaCO<sub>3</sub> samples prepared under the CIM and DPIM condition and calculated crystallinity values are shown in Table III. As shown in Figure 7, the melting peak of DPIM sample has a tendency to form the second high temperature peak. This shows

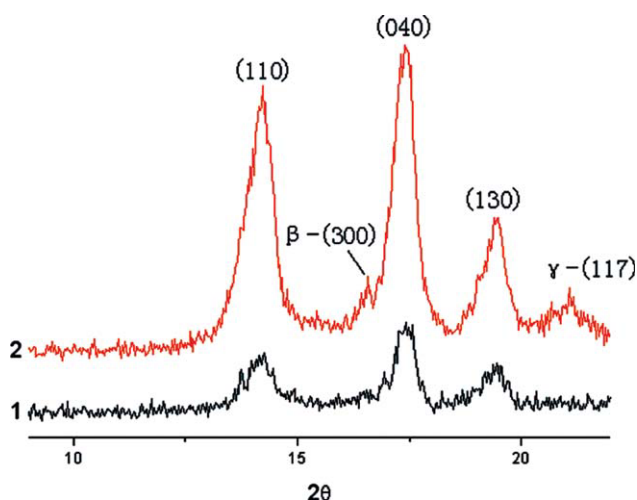


Figure 6 WAXD curves of CIM and DPIM samples shear layer. 1-CIM; 2-DPIM. [Color figure can be viewed in the online issue, which is available at [wileyonlinelibrary.com](http://wileyonlinelibrary.com).]

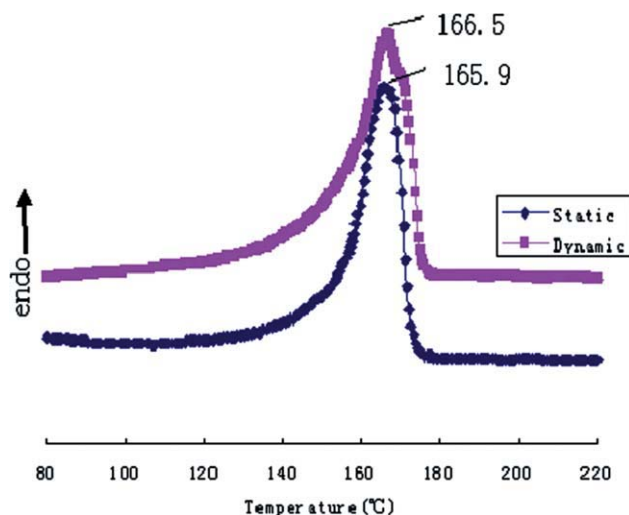


Figure 7 DSC curves of CIM and DPIM samples shear layer. [Color figure can be viewed in the online issue, which is available at [wileyonlinelibrary.com](http://wileyonlinelibrary.com).]

**TABLE III**  
DSC Results Obtained by CIM and DPIM Samples

Samples	Melting peak (°C)	$\Delta H_C$ (J g <sup>-1</sup> )	Crystallinity (%)
CIM	165.9	72.87	38.35
DPIM	166.5	116.1	61.11

that there might be shish-kebab structure to form.<sup>19,20</sup> The melting peak of DPIM sample is a little higher than that of CIM samples. This indicates that the lamellar thickness of PP has a small increase under the dynamic shear field. In addition, a large increase in fusion heat in DPIM samples is found compared with CIM samples. So the crystallinity of DPIM samples increases by 22.76% compared with CIM samples. On the one hand, the molecular chains of PP have certain ordered nature because they receive the periodic shear stretch function under the dynamic shear field before the crystallization. Reduction of the entropy is favorable to crystallize. Thus, the crystallization process is more perfect, and the crystallinity also improves. On the other hand, the dispersion of nano-CaCO<sub>3</sub> particles is even under the dynamic shear stress field. Nano-CaCO<sub>3</sub> particles can act as heterogeneous nucleating agent in PP/nano-CaCO<sub>3</sub> composites. They make PP crystal in a way of heterogeneous nucleation. Because of the even dispersion of nano-CaCO<sub>3</sub> in samples obtained by DPIM, the crystallinity of DPIM sample is higher than that of CIM sample.

### CONCLUSIONS

The conclusions of this work can be summarized as follows:

1. Dynamic packing injection molding (DPIM) technology can improve the mechanical properties of PP/nano-CaCO<sub>3</sub> samples significantly. Compared with conventional injection molding (CIM), the enhancement of the tensile strength and impact strength of the samples molded by DPIM was 39 and 144%, respectively. In addition, the tensile strength and impact strength of the PP/nano-CaCO<sub>3</sub> composites molded by DPIM increase by 21 and 514% respectively compared with those of pure PP through CIM.
2. Dynamic packing injection molding can allow more even dispersion of nano-CaCO<sub>3</sub> particles within PP/nano-CaCO<sub>3</sub> composites. The

agglomerated particles are broke up and dispersed homogenously by shear stress. This is one of the main reasons for improvement of impact strength and tensile strength of PP/nano-CaCO<sub>3</sub> composites obtained by DPIM.

3. Dynamic packing injection molding can change the microstructure and morphology of PP matrix. The crystallinity of DPIM samples increases by 22.76% compared with conventional samples. Moreover,  $\gamma$ crystal is found in the shear layer of the DPIM samples. The formation of  $\gamma$ crystal and increase of crystallinity are all favorable to the improvement of tensile strength of PP/nano-CaCO<sub>3</sub> DPIM samples.
4. Microscopic structure and morphology obtained by SEM, WAXD, and DSC analysis provide powerful evidence for explaining the reason for improvement of macroscopic mechanical properties of PP/nano-CaCO<sub>3</sub> composites by DPIM. The improvement of mechanical properties of PP/nano-CaCO<sub>3</sub> composites prepared by DPIM attributes to the even distribution of nano-CaCO<sub>3</sub> particles and the morphology change of PP matrix under the influence of dynamic shear stress.

### References

1. Wu, S.; Lian, E. *Rubber Industry* 1999, 46, 146.
2. Lee, I.; Han, S.W.; Hoi, H.J. *Adv Mater* 2001, 21, 1617.
3. Long, S.; Huang, R.; Yang, J. *Synthetic Resin Plast* 2004, 21, 77.
4. Oksuz, M.; Yildirim, H. *J Appl Polym Sci* 2005, 96, 1126.
5. Leong, Y. W.; Ishak, Z. A.; Mohd.; Ariffin, A. *J Appl Polym Sci* 2004, 91, 3327.
6. Akovali, G.; Akman, M. *Polym Int* 1997, 42, 195.
7. Supaphol, P.; Harnsiri, W.; Junkasem, J. *J Appl Polym Sci* 2004, 92, 201.
8. Guo, T.; Wang, L. *China Plast* 2004, 18, 23.
9. Ma, C.; Rong, M.; Zhang, M. *Acta Polym Sin* 2003, 44, 381.
10. Wan, W.; Yu, D.; Guo, X. *J Appl Polym Sci* 2006, 102, 3480.
11. Yan, H.; Pan, G.; Hu, Y. *Plast Industry* 2004, 32, 46.
12. Wang, X.; Huang, R. *China Plast* 1999, 13, 22.
13. Lei, J.; Jiang, C.; Shen, K. *J Appl Polym Sci* 2004, 93, 1584.
14. Chen, L.; Shen, K. *Polym Mater Sci Eng* 1999, 15, 87.
15. Avella, M.; Dell, R.; Martuscelli, E.; Ragosta, G. *Polymer* 1993, 34, 2951.
16. Qian, X.; Cheng, R.; Zhou, J.; Fang, W. *Plast Industry* 2003, 31, 24.
17. Hong, D. *Polypropylene-Principle, Art and Technology*. Petrochemical Pressing in China, 2002.
18. Li, Y.; Gao, X.; Yuan, Y.; Shen, K. *Acta Polym Sin* 2007, 12, 1111.
19. Chen, L.; Shen, K. *J Appl Polym Sci* 2000, 78, 1906.
20. Chen, L.; Shen, K. *J Appl Polym Sci* 2000, 78, 1911.